Arch. Metall. Mater. **67** (2022), 2, 587-594

DOI: https://doi.org/10.24425/amm.2022.137794

C. PANAGHIE[1], N. CIMPOESU[1*], M. BENCHEA[2], A.-M. ROMAN[1], V. MANOLE[1], A. ALEXANDRU[1], R. CIMPOESU[1], M.M. CAZACU[3], I. WNUK[4], G. ZEGAN[5]

"*IN-VITRO*" TESTS ON NEW BIODEGRADABLE METALLIC MATERIAL BASED ON ZnMgY

Biodegradable materials represent a new class of biocompatible materials with applications in many medical cases where the support must be provided only for a certain period. In this article obtaining of ZnMgY alloy is presented along with some basic characteristic investigations like chemical composition (energy dispersive spectroscopy – EDS), microstructure (optical microscopy – OM and scanning and electron microscopy – SEM), immersion behavior in 10xDPBS (Dulbecco Phosphate Buffer Saline) solution (mass loss and surface degradation), electro-corrosion behavior (potentiostat with a three electrodes cell) and micro-hardness of the experimental alloy compared to cast Zn and ZnMg materials. The results present an improvement of micro-hardness of Zn by alloying with Mg and Y and a modification of corrosion resistance.

Keyword: Biodegradable; Tafel; Potentiostat; Micro-hardness; 10xDPBS

1. Introduction

Besides well-known magnesium based biodegradable alloys and iron-based materials a novel system gains much attention for medical applications with degradation period between those of Mg and Fe, which are based on zinc. The main concern on zinc application is based on his poor mechanical properties [1]. Passing the years, technology and science have evolved. The desire of researchers was to find the most modern and advanced materials to meet the demand and needs of a 21st-century lifestyle. The scope is to use them in industrial or medical fields. For the medical field, researchers are trying to develop materials for implants with the best performance possible starting from good mechanical properties, good wear resistance, to biodegradability and biocompatibility [2].

The concept of biodegradability has been studied extensively. A good biodegradable material must gradually corrode "in vivo" (have a corrosion resistance), the host need to eliminate products from corrosion and decompose completely after fulfilling its purpose. A great advantage of the biodegradable implant is that it does not require the second surgery after the end of implantation, saving pain, time and money [3].

The method for obtaining and processing biomaterials has a great influence on their quality. Methods of obtaining have been developed starting from the classic ones [4-6] such as casting, rolling, extrusion, drawing to advanced ones such as severe plastic deformation, additive manufacturing [7,8]. Materials such as Mg and Fe and their alloys have been studied extensively and are already used in various medical applications [9]. Zinc was the last to be studied to balance the disadvantages of iron and magnesium [10,11].

Zinc is an element with an important role in the human body. The body of a human adult contains 2-3 grams of zinc having different biological functions with an important role from enzymatic catalysis to neuronal systems [12]. Pure zinc has an ideal corrosion behavior but weak mechanical properties. Studies on Zn alloy as a biodegradable material were reported since 2007, when Wang et.al analyzed mechanical properties and degradation behavior in SBF solution. Another researcher was Bowen et.al, who studied pure zinc wire by implanting it into the blood vessel, and his study reveals that zinc had good corrosion behavior for biodegradable stents [13].

By alloying it with different metals it is tried to improve the properties, obtaining results close to those of Fe-based or

[1] GHEORGHE ASACHI UNIVERSITY OF IASI, FACULTY OF MATERIALS SCIENCE ENGINEERING, PROF.DR.DOC. D. MANGERON STR., NO. 41, IAŞI 700050, ROMANIA
[2] GHEORGHE ASACHI UNIVERSITY OF IASI, FACULTY OF MECHANICAL ENGINEERING, PROF.DR.DOC. D. MANGERON STR., NO. 61-63, IAŞI 700050, ROMANIA
[3] GHEORGHE ASACHI UNIVERSITY OF IASI, DEPARTMENT OF PHYSICS, PROF.DR.DOC. D. MANGERON STR., NO. 59A, IAŞI 700050, ROMANIA
[4] CZĘSTOCHOWA UNIVERSITY OF TECHNOLOGY, DEPARTMENT OF PHYSICS, 19 ARMII KRAJOWEJ AV., 42-200 CZĘSTOCHOWA, POLAND
[5] GRIGORE T. POPA UNIVERSITY OF MEDICINE AND PHARMACY, FACULTY OF DENTAL MEDICINE, UNIVERSITY STR., NO. 16, IAŞI 700115, ROMANIA
* Corresponding author: nicanor.cimpoesu@tuiasi.ro

Mg-based alloys [14-16]. Systems like Zn-Mg, Zn-Cu, Zn-Fe, Zn-Ag, Zn-Mn, Zn-Ca, Zn-Sr, Zn-Li were studied for bone implants, from "in vitro" to "in vivo" perspective [17]. For better results the third element was considered, and systems such as ZnMgZr were already studied [18]. Referring to the Zn-Mg binary system, by adding the Y element we intend to improve the corrosion behavior and mechanical properties. No studies have been found on this ternary system.

Experimental tests were performed on a new ZnMgY cast alloy in order to determine the influence of addition elements (Mg and Y) on pure Zn mechanical and corrosion resistance characteristics.

TABLE 1

Chemical composition of the ingots (average values from five determinations)

Materials/ elements	Zn		Mg		Y	
	wt%	at%	wt%	at%	wt%	at%
Zn pure	99.99	99.99	—	—	—	—
Zn3Mg	97.04	91.60	2.96	7.26	—	—
Zn3Mg0.7Y	96.35	86.25	2.94	6.80	0.71	0.60
EDS error	1.2		0.3		0.1	

St. Dev. (made from ZnMgY alloy chemical composition determinations): Zn÷1.9, Mg÷0.1, Y÷0.1

2. Materials and methods

2.1. Elaboration process

Three samples (Zn, Zn3Mg and Zn3Mg0.7Y) were obtained by casting in an induction furnace with argon atmosphere, in Fig. 1 details of the casting and pouring process were presented. Materials used were pure Zn, Mg pure and MgY as master alloy in a proportion of 70%Mg and 30%Y wt% [19]. After calculating the loading batches, the following quantities were used: for Zn probe –100 grams of Zn with high purity, for the Zn3Mg alloy –97 grams Zn and 3 grams Mg was used, and for the experimental alloy Zn3Mg0.7Y –97 grams Zn were used, 2.35 grams of master alloy and 1.35 grams of pure Mg.

To obtain a better homogeneity of the alloys, the batches were three times re-melted. We obtained ~100 grams' ingots that were subsequently mechanically processed, cut, polished with granulation starting from 500 up to 2000 grid and ultrasound cleaned to be analyzed. Experimental ingots present the chemical composition from TABLE 1 (mass and atomic percentages) with values near the proposed ones.

To verify the efficiency of the remelting and confirmation of the homogenization the samples were tested with fluorescent penetrating liquids. This type of test revealed discontinuities, porosities, cracks or inclusions in the material. Method used was hydrophilic post-emulsify. Penetrant liquid used was an ultra-high sensitivity level four and hydrophilic emulsifier in concentration of 6-7%. For a good contrast we used a dry developer to amplify the indications. Main steps of the process were: dwell time of penetration – 30 minutes, emulsification time – 3 minutes, developer time – 15 minutes. The inspection was done under the ultraviolet light with intensity of 3500 $\mu W/cm^2$ measured at 38 cm distance. The surface state of the cast materials is shown in Fig. 2 before and after the re-melting process.

After re-melting, Fig. 2(b), a big part of the pores, inclusions or micro-cracks were removed, improving the surface quality of the material, an extremely important condition for implantable materials success.

The entire elaboration process as well as the tests mentioned above were carried out with protective equipment, in safe conditions and under the supervision of the laboratory manager [20-21].

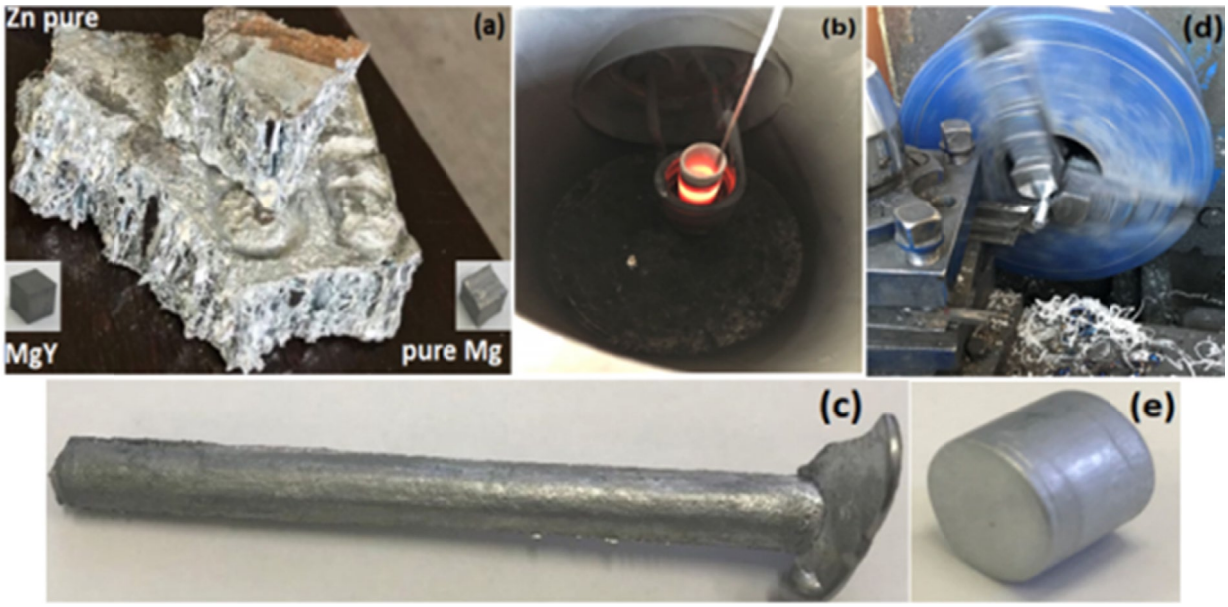

Fig. 1. Manufacturing process: (a) materials used, (b) induction furnace, (c) ingot, (d) lathe machine, (e) final product

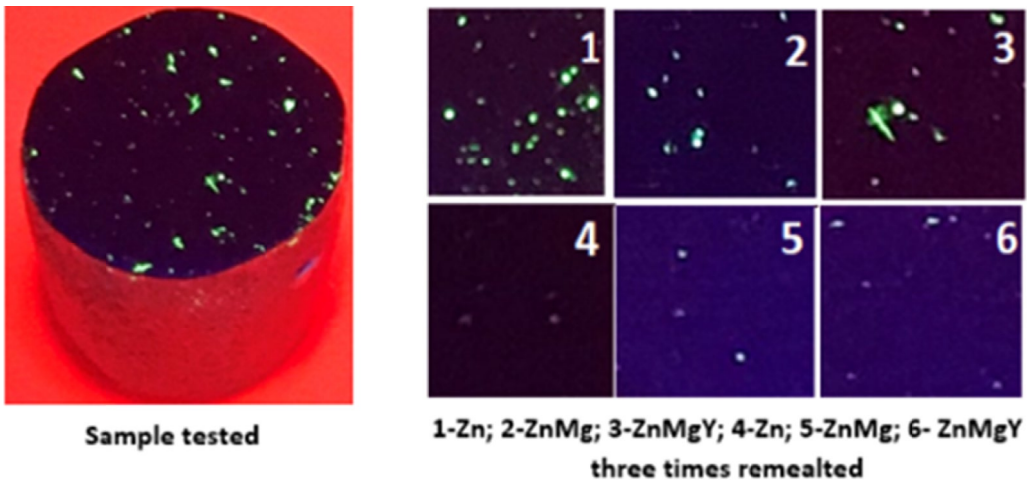

Fig. 2. Cast material surface after NDT test using penetrant liquids (a) before and (b) after five times re-melting

2.2. Microhardness investigation

Universal Micro-Tribometer equipment was used for testing Zn pure, Zn3Mg and Zn3M0.7Y samples (50×10×5 mm) with different Friction/Load sensors varying in range and sensitivity. Tests were made with Rockwell diamond tip with 120° opening angle. Standard dimensions of the Rockwell tip indenter are: –radius of 200 ±5 μm; angle – 120° ±0.30 and standard deviation from the median line of ±2 μm. The software used was UTM Viewer, a program that translates data files produced with the UTM testing software into graphical display for analysis. Data files are in binary form. "Textify" will create an ASCII text version of the file for importing to spreadsheet programs. Using the OriginPro software the excel file can be imported and a graph was plotted.

2.3. Corrosion resistance tests

Electro-corrosion resistance was analyzed with VoltaLab-21 potentiostat that helps us investigate the linear and cyclic potentiometry in 10xDPBS (free Ca and Mg Dulbecco's solution) with chemical composition: KCl: 0.2; KH_2PO_4:0.2; NaCl: 8.0; $NaHPO_4$ (anhydrous):1.15). Laboratory equipment containing three electrode cells and an auxiliary platinum electrode and calomel saturated were used. The tests were made at 23°C (room temperature) and the results were plotted as current density [mA/cm^2] function of potential [V]. Using VegaTescan LMH II SEM, we investigate the surface and microstructure of the samples after electro-corrosion testing and chemical composition with Bruker – EDS detector.

3. Results and Discussion

3.1. Chemical analysis of the experimental alloy

After casting the material chemical composition analysis was performed on Zn3Mg0.7Y alloy. Experimental results, Fig. 3, present a homogeneous distribution of the main elements, respectively Zn, Mg and Y with characteristic X-ray energy values presented in Fig. 2(a). The microstructure of ZnMgY alloy, Fig. 2(b), is a typically dendritic structure. The cast alloy is formed by a matrix and eutectic combination of Zn+Mg_2Zn_{11}. Besides the solid solution based on Zn and MgZn compounds, other compounds were observed having different morphologies like YZn12 and Mg12ZnY [22].

The compounds based on ZnY and MgZnY present an important role in hardness modification of pure Zn [23]. The spread of these compounds will also affect the material mechanical characteristics and can influence the corrosion rate by forming galvanic micro-cells. In Fig. 3(e), an agglomeration of Y can be observed, which is characteristic to YZn_{12} compound and which have 10% wt Y percentage and the rest is 90%wt Zn more than all other compounds formed on ZnMgY alloy or in Zn based solid solution.

3.2. Microhardness tests

All the sample were tested through micro-hardness Rockwell test, and average values from five determinations presented in TABLE 2. Zinc is a soft material with HCP-hexagonal close-packed crystal structure and low melting point. Following the results obtained and highlighted in TABLE 2, we concluded that the lowest hardness is for Zn pure, an expected result based on specialty literature [23]. The difference in microhardness between pure Zn and ZnMg or ZnMgY alloys is significant (an increase of hardness of 6.6 bigger for ZnMgY) considering really small percentages used for addition (~3%wt Mg and 0.7%wt Y). This confirms that the addition of yttrium as the third element also increases the value of hardness. Fig. 4 represents load-depth variation graphs of the sample behavior.

The main characteristics given by Rockwell micro-hardness indentation test, TABLE 2, present an important improvement in hardness with the addition of Mg to pure Zn and a supplementary increase with alloying with Y. Both Young modulus and contact

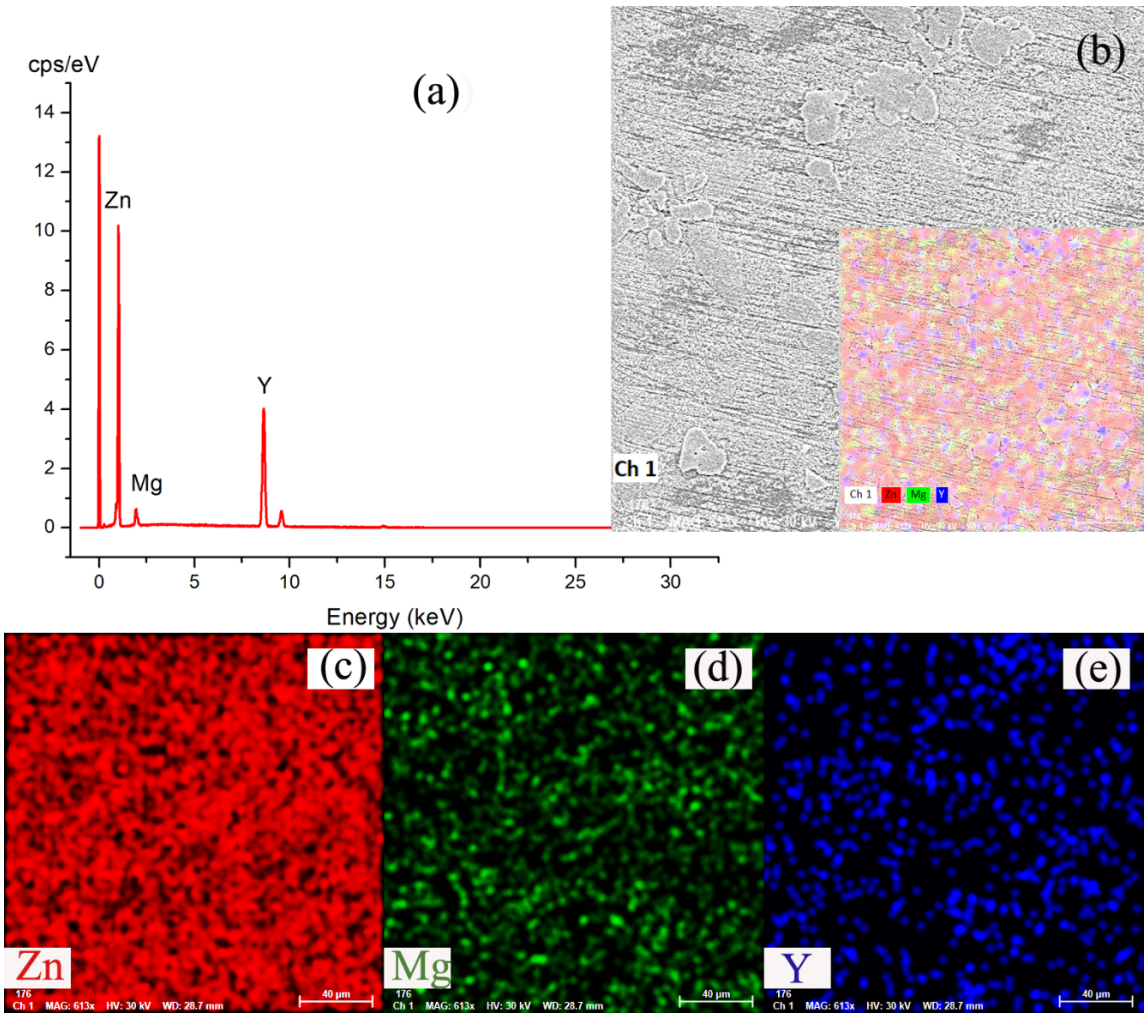

Fig. 3. Chemical analysis of the experimental alloy ZnMgY (a) energy spectrum, (b) ZnMgY element distribution, (c) Zn distribution, (d) Mg distribution, (e) Y distribution

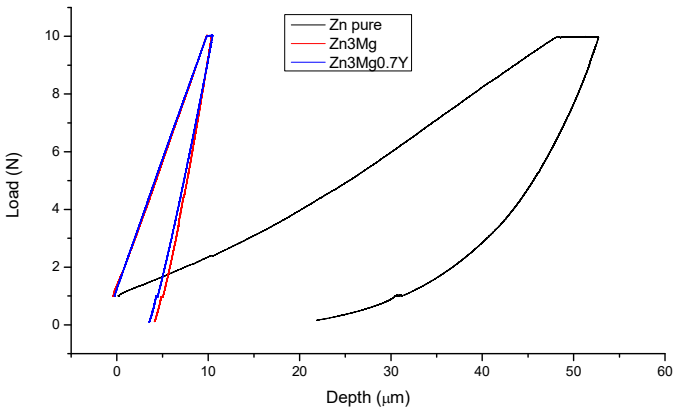

Fig. 4. Microhardness results of pure Zn, ZnMg and Zn3Mg0.7Y

stiffness greatly increase with the addition of Mg and slowly decrease with the addition of Y in comparison to ZnMg sample.

Mechanical properties are considered one of the main problems of using Zn as biodegradable material and with the addition of Mg, part of the properties are obviously improved. Furthermore, with the addition of Y a higher hardness was obtained, and a less contact stiffness compared to ZnMg.

3.3. Immersion and electro-corrosion tests

Zinc presents a good corrosion resistance because of the passive layers formed by corrosion products on top of the surface

TABLE 2

Mechanical characteristics of as-cast samples made through Rockwell indentation (average values from five determinations)

Sample	Indentation Modulus Young [GPa]	Hardness [GPa]	Maximum Load [N]	Maximum Displacement [μm]	Contact stiffness [N/μm]	Contact depth [μm]	Contact area [μm^2]
Zn pure	2.90	0.17	8.95	52.53	0.82	44.68	53890.63
ZnMg	17.34	0.98	9.02	10.82	2.01	7.44	9175.23
Zn3Mg0.7Y	15.07	1.10	9.03	10.74	1.65	6.62	8180.18

during contact with the electrolyte solution. Zinc-magnesium system alloys were used in the previous years as corrosion-resistant coatings for Fe-C alloys [24]. The immersion and electrolyte solution used in this experiment are the same Mg and Ca-free solution (10xDPBS) so the Mg percentages appeared is due to the alloy contribution. Alloying with Mg seems to improve the corrosion resistance of Zn. Element Mg presence in compounds (intermetallic phases) change the chemical composition of degradation film growth in the first days of corrosion. The thin films made of MgO, present a higher protective effect compared to ZnO based on their smaller electrical conductivity [25]. Simonkoleite: $Zn_5(OH)_8Cl_2$-H_2O is a usual corrosion compound on Zn-Mg surface and gives better protection than ZnO-based compounds appearing on pure Zn [26].

The samples were immersed in 10xDPBS solution at a temperature of 37 ±1°C and kept for 24, 48 and 72 hours. They were weighed before, after immersion and after ultrasonic cleaning to highlight the weight variation, mass differences are given in TABLE 3. Weight gain of 1-2.2 mg was observed due to the reaction between the 10xDPBS solution and the material.

TABLE 3

Mass variations of the sample after immersion (24, 48 and 72 hours) in 10xDPBS and ultrasound cleaning

Sample		Initial weight [g]	Weight after immersion [g] (mg)	Weight after ultrasound cleaning [g](mg)
Zn	24H	4.1888	4.1906 (+1.8)	4.1902 (+1.4)
	48H	3.9416	3.9438 (+2.2)	3.9431 (+1.5)
	72H	4.1369	4.1391 (+2.2)	4.1387 (+1.8)
ZnMg	24H	2.6388	2.6410 (+2.2)	2.6401 (+1.3)
	48H	3.4378	3.4394 (+1.6)	3.4386 (+0.8)
	72H	2.4310	2.4328 (+1.8)	2.4326 (+1.6)
Zn3Mg0.7Y	24H	2.4484	2.4501 (+1.7)	2.4496(+1.2)
	48H	2.9427	2.9437 (+1.0)	2.9434 (+0.7)
	72H	1.7236	1.7258 (2.20)	1.7253 (+1.7)

In our study, ZnMgY alloy, the growth and formation of intermetallic phases (Mg_2Zn_{11}, YZn_{12}, or $Mg_{12}ZnY$) will increase the galvanic corrosion effect between generally Zn matrix (with reduced percentages of Mg and Y dissolved in Zn matrix) and mentioned compounds in the eutectic region. Because magnesium presents a higher activity than zinc [27,28], will be extracted from the alloy and the release of Mg^{2+} and OH^- ions (Eq. 6). Then, Mg containing products, such as $Mg(OH)_2$, Mg-CO_3 and Mg-PO_4, pass from alloy surface to the electrolyte solution, especially after ultrasound cleaning of the samples. Mainly product growth on the surface after immersion or electro-corrosion experiments can be the mixtures of $Zn(OH)_2$, $Mg(OH)_2$, Zn/Mg-CO_3 and Zn/Mg/PO_4, which can be verified by TABLE 4.

All samples present a high percentage of oxidation (26-30%wt), and the presence of phosphorus on the surface confirms the formation of phosphate compounds and their adhesion to the metallic surface. Few stains of salts (K present) or Cl-based compounds were also identified on the surface. Both Mg and Y elements present smaller percentages than the initial composition, TABLE 1, the chemical composition being influenced by the corrosion process and the compound formation after the interaction between the alloy and electrolyte solution.

3.4. Electrochemical polarization test

This method establishes the form of corrosion and anodic or cathodic protection [27]. The electrolyte solution was continuously stirred to avoid bubble formation on the metallic surface. Nevertheless, comparing to magnesium alloys there is a much smaller hydrogen quantity release during corrosion of the material, an advantage towards Mg-base alloys. The linear and cyclic curves presented in Fig. 5(a) and (b) present a similar behavior of Zn, ZnMg and ZnMgY cast alloys with a generalized corrosion allure of the cyclic curves.

Surface state of the samples after electro-corrosion experiments and ultrasound cleaning for 60 minutes in alcohol made by SEM, Fig. 6(a)-(c), confirm the generalized behavior of the electro-corrosion. The surface of pure Zn looks like chemical etching, highlighting the grains microstructure. In all samples case a small number of compounds remain attached to the surface probably oxides, hydroxides or phosphates. Pitting type agglomerations of holes can be observed on Zn and ZnMgY alloys that will accelerate the degradation of the material.

The influence of Y on the corrosion resistance of Zn_3Mg-Y -based alloys is a complex process, by one side, the percentage of Y participates in the formation of YZn_{12} intermetallic phase elements, with a more noble potential than pure Zinc [28] and showing a more aggressive galvanic corrosion between Mg_2Zn_{11} and YZn_{12} with the Zn matrix, Fig. 6(c). At micrometric scale, this difference can increase the localized corrosion of the ternary alloys compared to pure Zn or binary ZnMg alloys. As a second thinking the presence of Y has a homogenization role of the

TABEL 4

Chemical composition of the test samples after 3 days' immersion in 10xDPBS solution and ultrasound cleaning

Material	Zn		Mg		Y		O		P		Cl		K	
	wt%	at%	wt%	at%	wt%	at%	wt%	at%	wt%	at%	wt%	at%	wt%	at%
Zn pure	96.95	92.2	—	—	—	—	28.76	57.17	12.88	13.23	2.93	2.63	—	—
Zn3Mg	55.42	26.97	1.09	1.38	—	—	29.91	57.45	15.66	15.54	—	—	1.74	1.37
Zn3Mg0.7Y	51.28	23.96	0.67	0.85	0.25	0.09	30.65	58.51	15.70	15.48	—	—	1.44	1.12
EDS error	1.1		0.2		0.1		0.9		0.7		0.2		0.1	

Standard Deviation: Zn:±1.5, Mg: ±0.15, Y: ±0.1, O: ±2, P: ±0.5, Cl: ±0.15 and K: ±0.2

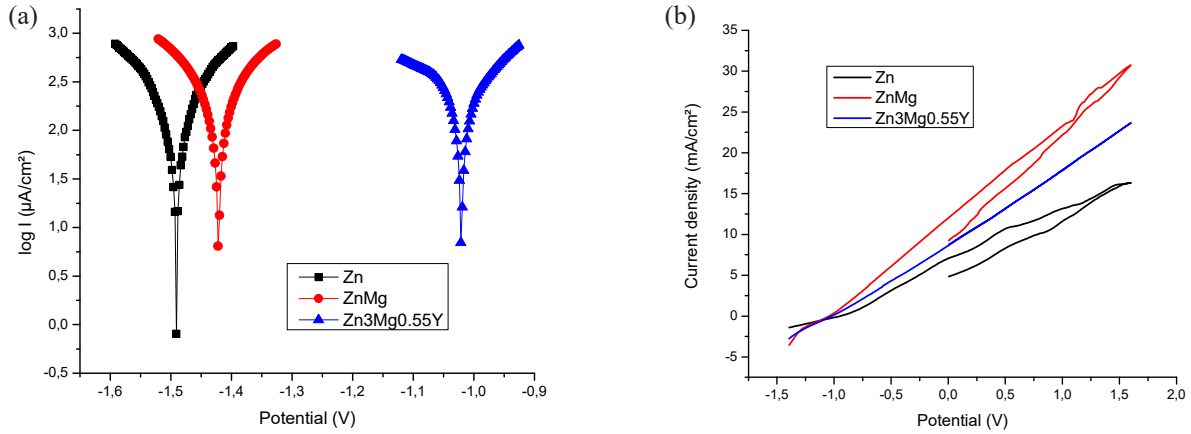

Fig. 5. Linear and cyclic potentiometry: (a) Tafel diagram, (b) cyclic potentiometry

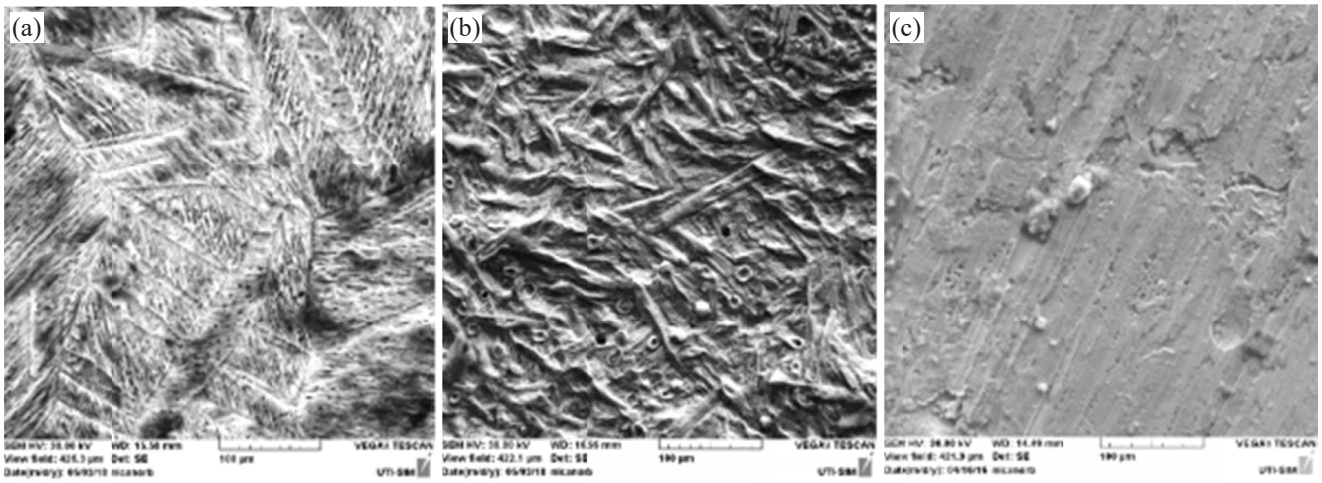

Fig. 6. Structure after three days of immersion and ultrasound cleaning: (a) Zn, (b) Zn3Mg and (c) ZnMg0.7Y

microstructure and can increase corrosion resistance based on the growth of an uninterrupted layer on the surface, resulting in a better corrosion resistance of the surface film formed during immersion. Both the anodic and cathodic processes are almost equal meaning that the chemical reactions are intense on both reduction and oxidation parts during the electro-corrosion.

Two cathodic reactions occurred during electro-corrosion tests [29-31]:

$$2H_2O + 2e^- \rightarrow H_2 + 2OH^- \quad (1)$$

$$2H_2O + O_2 + 4e^- \rightarrow 4OH^- \quad (2)$$

and more anodic reactions:

$$2Zn \rightarrow 2Zn^{2+} + 4e^- \quad (3)$$

$$Zn^{2+} + CO_3^{2-} \rightarrow ZnCO_3 \quad (4)$$

$$Zn^{2+} + PO_4^{3-} \rightarrow Zn\text{-}PO_4 \quad (5)$$

$$Mg \rightarrow Mg^{2+} + 2e^- \quad (6)$$

From TABLE 5 results we observed that the micro-galvanic cells accelerate localized corrosion, increasing the corrosion rate of the tertiary alloy even the amount of Y is small. In case of immersion, the homogeneous microstructure is likely to play the dominant roles in the corrosion behavior of the alloys, as supported by the enhanced passivation performance and the increased corrosion resistance of the samples in first days of immersion in 10xDPBS.

Mg and Y elements presents an important role in the corrosion process of ZnMgY alloys and are influenced by Mg and

TABLE 5

Electro-corrosion resistance parameters of the samples in 10xDPBS electrolyte

Sample	E_0 mV	b_a mV	b_c mV	R_p ohm.cm²	J_{corr} μA/cm²	V_{corr} mm/Year
Zn	–1491.4	122.2	–141.1	168.97	159.81	1.79
Zn Mg	–1469.8	106.0	–132.0	167.01	138.33	1.55
Zn3Mg0.7Y	–1020.4	145.4	–95.8	108.61	175.07	1.97

Y-rich intermetallic phases that acts in the microstructure as the anodic sites and therefore dissolve preferentially to form Mg^{2+} or Y^{2+} cations, which move further the cathodic sites. As a result, especially Mg hydroxide- and Mg carbonate-based compounds are formed at cathodic sites, which react with OH^- anions. These compounds tampon the corrosive environment, thereby slowing the O_2 reduction and the formation of ZnO.

4. Conclusions

A new ZnMgY material was obtained through induction casting. The material presents an increase of mechanical properties, an increase in microhardness more than five times comparing to pure Zn (1.10 for ZnMgY compared to 0.17 for Zn). Young modulus (15.07 for ZnMgY compared to 2.9 for Zn) and materials stiffness (1.65 for ZnMgY compared to 0.82 for Zn) were also enhanced by the addition of Mg and Y in pure Zn matrix. During the immersion of the samples (pure Zn, ZnMg alloy and ZnMgY) a phosphate layer (from the interaction with 10xDPBS solution) is formed on the surface with a protective role at least in the first three days of immersion. At electro-corrosion, the intermetallic compounds formed in ZnMgY alloy have an important role in corrosion resistance through galvanic micro-cells that appear during the test and increase the degradation rate of the sample however comparable with the corrosion rate of pure Zn (1.97 for ZnMgY compared to 1.79 for Zn).

Acknowledgments

A part of this work was supported by a grant of the Romanian Ministry of Education and Research, CNCS - UEFISCDI, project number PN-III-P1-1.1-TE-2019-1921, within PNCDI III.

REFERENCES

[1] H. Yang, B. Jia, Z. Zhang, X. Qu, G. Li, W. Lin, D. Zhu, K. Dai, Y. Zheng, Alloying design of biodegradable zinc as promising bone implants for load-bearing applications, Nature Communications **11**, 401 (2020).

[2] H. Hermawan, Biodegradable Metals: State of the Art, Biodegradable Metals, Springer (2012).

[3] Y.F. Zheng, X.N. Gu, F. Witte, Mat. Sci. Eng. R **77**, 1-34 (2014).

[4] A.V. Sandu, M.S. Baltatu, M. Nabialek, A. Savin, P. Vizureanu, Characterization and Mechanical Proprieties of New TiMo Alloys Used for Medical Applications, Materials **12** (18), 2973 (2019). DOI: https://doi.org/10.3390/ma12182973

[5] S. Zhao, J.M. Seitz, R. Eifler, H.J. Maier, R.J. Guillory, E.J. Earley, A. Drelich, J. Goldman, J.W. Drelich, Mater. Sci. Eng. C **76**, 301-312 (2017).

[6] M.S. Baltatu, P. Vizureanu, A.V. Sandu, C. Munteanu, B. Istrate, Microstructural Analysis and Tribological Behavior of Ti-Based Alloys with a Ceramic Layer Using the Thermal Spray Method, Coatings **10** (12), 1216 (2020). DOI: https://doi.org/10.3390/coatings10121216

[7] M.S. Dambatta, S. Izman, D. Kurniawan, H. Hermawan, Processing of Zn-3Mg alloy by equal channel angular pressing for biodegradable metal implants, J. King Saud Univ. Sci. **29** (4), 455-461 (2017).

[8] P. Vizureanu, M. Nabialek, A.V. Sandu, B. Jez, Investigation into the Effect of Thermal Treatment on the Obtaining of Magnetic Phases: Fe5Y, Fe23B6, Y2Fe14B and alpha Fe within the Amorphous Matrix of Rapidly-Quenched Fe61+xCo10-xW1Y8B20 Alloys (Where x=0, 1 or 2), Materials **13** (4), 835 (2020). DOI: https://doi.org/10.3390/ma13040835

[9] H.F. Li, Z.Z. Shi, L.N. Wang, Opportunities and challenges of biodegradable Zn-based alloys, Journal of Materials Science & Technology **46**, 136-138 (2020).

[10] P.K. Bowen, J. Drelich, J. Goldman, Zinc exhibits ideal physiological corrosion behavior for bioabsorbable stents, Adv. Mater. **25**, 2577-2582 (2013).

[11] D. Vojtech, J. Kubasek, J. Serak, P. Novak, Mechanical and corrosion properties of newly developed biodegradable Zn-based alloys for bone fixation, Acta Biomater. **7**, 3515-3522 (2011).

[12] K. Kaur, R. Gupta, S.A. Saraf, S.K. Saraf, Zinc: the metal of life, Compr. Rev. Food Sci. Food Saf. **13** (4), 358-376 (2014).

[13] G. Li, H. Yang, Y. Zheng, X.H. Chen, J.A. Yang, D. Zhu, L. Ruan, K. Takashima, Challenges in the use of zinc and its alloys as biodegradable metals: Perspective from biomechanical compatibility Acta Biomaterialia, **97**, 23-45 (2019).

[14] S. Zhao, J.M. Seitz, R. Eifler, H.J. Maier, R.J. Guillory 2nd, E.J. Earley, A. Drelich, J. Goldman, J.W. Drelich, Zn-Li alloy after extrusion and drawing: structural, mechanical characterization, and biodegradation in abdominal aorta of rat, Mater. Sci. Eng. C Mater. Biol. Appl. **76**, 301-312 (2017).

[15] J. Niu, Z. Tang, H. Huang, J. Pei, H. Zhang, G. Yuan, W. Ding, Research on a Zn-Cu alloy as a biodegradable material for potential vascular stents application, Mater. Sci. Eng. C Mater. Biol. Appl. **69**, 407-413 (2016).

[16] H.F. Li, X.H. Xie, Y.F. Zheng, Y. Cong, F.Y. Zhou, K.J. Qiu, X. Wang, S.H. Chen, L. Huang, L. Tian, L. Qin, Development of biodegradable Zn-1X binary alloys with nutrient alloying elements Mg, Ca and Sr, Sci. Rep. **5**, 10719 (2015).

[17] H. Yang, B. Jia, Z. Zhang, X. Qu, G. Li, W. Lin, D. Zhu, K. Dai, Y. Zheng, Alloying design of biodegradable zinc as promising bone implants for load-bearing applications, Nature Communications **11**, 401 (2020).

[18] T. Ren, X. Gao, C. Xu, L. Yang, P. Guo, H. Liu, Y. Chen, W. Sun, Z. Song, Evaluation of as-extruded ternary Zn-Mg-Zr alloys for biomedical implantation material: In vitro and in vivo behavior, Materials and Corrosion, (2018). DOI: https://doi.org/10.1002/maco.201810648

[19] Hunan High Broad New Material, Co.Ltd. Available online: http://www.hbnewmaterial.com/supplier-129192-master-alloy (accessed on 10 June 2019).

[20] M.A. Bernevig-Sava, D.C. Darabont, M. Lohan, E. Mihalache, C. Bejinariu, Selection and verification of personal protective

equipment in the context of current legal requirements, Quality – Access to Success **20**, 109-112 (2019).

[21] C. Baciu, C. Bejinariu, D.C.Darabont, A. Corăbieru, M.A. Bernevig-Sava, Occupational safety and health audit between theory, legal requirements and practice, Quality – Access to Success **20**, 113-116 (2019).

[22] J. Zhu, X.H. Chen, L. Wang, W.Y. Wang, Z.K. Liu, J.X. Liu, X.D. Hui, High strength Mg-Zn-Y alloys reinforced synergistically by Mg12ZnY phase and Mg3Zn3Y2 particle, J. Alloy Compd. **703**, 508-516 (2017).

[23] M. Dias, C. Brito, F. Bertelli, O. L. Rocha, A. Garcia, Interconnection of thermal parameters, microstructure, macrosegregation and microhardness of unidirectionally solidified Zn-rich Zn-Ag peritectic alloys, Materials and Design **63**, 848-855 (2014).

[24] C. Yao, Z. Wang, S. L. Tay, T. Zhu, Wei Gao, Effects of Mg on microstructure and corrosion properties of Zn-Mg alloy, Journal of Alloys and Compounds **602**, 101-107 (2014).

[25] G. Kastiukas, X. Zhou, ASCE, M., Babar Neyazi, K.T. Wan, Sustainable Calcination of Magnesium Hydroxide for Magnesium Oxychloride Cement Production, J. Mater. Civ. Eng. **31** (7), (2019).

[26] W. Gu, S. Zhai, Z. Liu, F. Teng, Effect of coordination interaction between water and zinc on photochemistry property of Zn3(PO4)2·2H2O, Chemical Physics **536**, 110811 (2020).

[27] Tables of Standard Electrode Potentials: by G. Milazzo and S. Caroli, John Wiley, Chichester and New York, 1978, pp. xvi +421, price £17.50, J. Mol. Struct. **54**, 307e308, (1979). DOI: https://doi.org/10.1016/0022-2860(79)80084-8

[28] G. Shao, V. Varsani, Z. Fan, Thermodynamic modelling of the Y-Zn and Mg-Zn-Y systems, Calphad. **30**, 286-295 (2006). (2020).

[29] D.P. Burduhos-Nergis, P. Vizureanu, A.V. Sandu, C. Bejinariu, Evaluation of the Corrosion Resistance of Phosphate Coatings Deposited on the Surface of the Carbon Steel Used for Carabiners Manufacturing, Applied Sciences-Basel. **10** (8), 2753 (2020).

[30] H. Zhou, R. Hou, J. Yang, Y. Sheng, Z. Li, L. Chen, W. Li, X. Wang, Influence of Zirconium (Zr) on the microstructure, mechanical, properties and corrosion behavior of biodegradable zinc-magnesium alloys, J. Alloy. Compd. **840**, 155792.

[31] D.P. Burduhos-Nergis, A.V. Sandu, D.D. Burduhos-Nergis, D.C. Darabont, R.I. Comaneci, C. Bejinariu, Shock Resistance Improvement of Carbon Steel Carabiners Used at PPE, MATEC Web Conf. **290**, 12004 (2019). DOI: https://doi.org/10.1051/matecconf/201929012004